Int J Clin Exp Med 2018;11(6):5764-5773
www.ijcem.com /ISSN:1940-5901/IJCEM0067498

Original Article

Development and characterization of experimental models of oligometastatic and polymetastatic progression

Zhiwei Sun*, Shixia Zhou*, Junling Tang, Ting Ye, Jingyuan Li, Jianyu Wang#, H Rosie Xing#

*Laboratory of Translation Cancer Stem Cell Research, Institute of Life Sciences, Chongqing Medical University, Chongqing, P.R. China. *Equal contributors. #Co-senior authors.*

Received June 15, 2017; Accepted March 13, 2018; Epub June 15, 2018; Published June 30, 2018

Abstract: Clinical oligometastases are characterized by a limited number of metastases which are a form of stable metastatic dissemination that presents the window for curative treatment. A better understanding of the molecular mechanisms underlining the differences between the stable oligometastases from the widespread polymetastases requires the development of clinically-relevant animal models for mechanistic investigation. In this study, we created from a MDA-MB-435 human tumor, the first mouse xenograft model of oligo- and polymetastases. Here, using this novel xenograft model to study two distinct types of metastatic progression, we report detailed characterization of experimental oligo- and polymetastases models. The oligometastatic model remained stable after serial rounds of *in vivo* passage, had limited organ involvement and had less than 5 discrete metastatic foci. In contrast, the polymetastatic progression model showed multiple metastatic foci in the lung, or involved multiple anatomic sites. In summary, the new xenograft models of metastasis that we reported here recapitulated phenotypic features of two clinically relevant human metastasis phenotypes: the oligometastatic and polymetastatic progression. These models should prove useful for mechanistic investigation as well as for evaluating therapeutic targeting of sustained oligometastases to achieve the clinical goal of long-term disease free survival.

Keywords: Oligometastases, polymetastases, metastasis, MDA-MB-435

Introduction

Metastases are the leading cause of cancer related mortality. However clinical studies have demonstrated the effectiveness of metastasis-directed therapies such as surgery or radiotherapy in treating patients exhibiting a limited number of metastases, i.e. oligometastases progression [1-11]. Approximately 75% of patients, initially presenting with limited metastases, will progress to a widespread metastatic state. We and our collaborators reported prioritized features of a potential microRNA classifier associated with a true oligometastatic state (cured or remain <5 metastases after metastasis directed treatment) in patients who presented with 5 or less metastases before being treated with stereotactic body radiotherapy (SBRT) [12]. These clinical observations suggest that molecular differences exist between tumors that remain oligometastatic following treatment and tumors that progress to polymetastases.

Characterization of oligometastases depends on identifying mechanisms regulating distinctive metastatic disease states. Most existing organ-specific experimental or spontaneous models of metastases investigate extensive metastatic dissemination [13-23]. Models that exhibit multiple-organ involvement are rare. Animal models that are specific to undergo oligometastatic progression are lacking. In a related model, Fidler et al demonstrated a spectrum of the number of lung metastatic foci formation following tail-vein-injection of single-cell derived clones of B16F1 melanoma [23-26]. They observed that while the majority of B16 monoclonal cell lines rapidly developed polymetastatic foci in the lungs, a limited number of B16 clones yielded a small number of lung metastases [24-26].

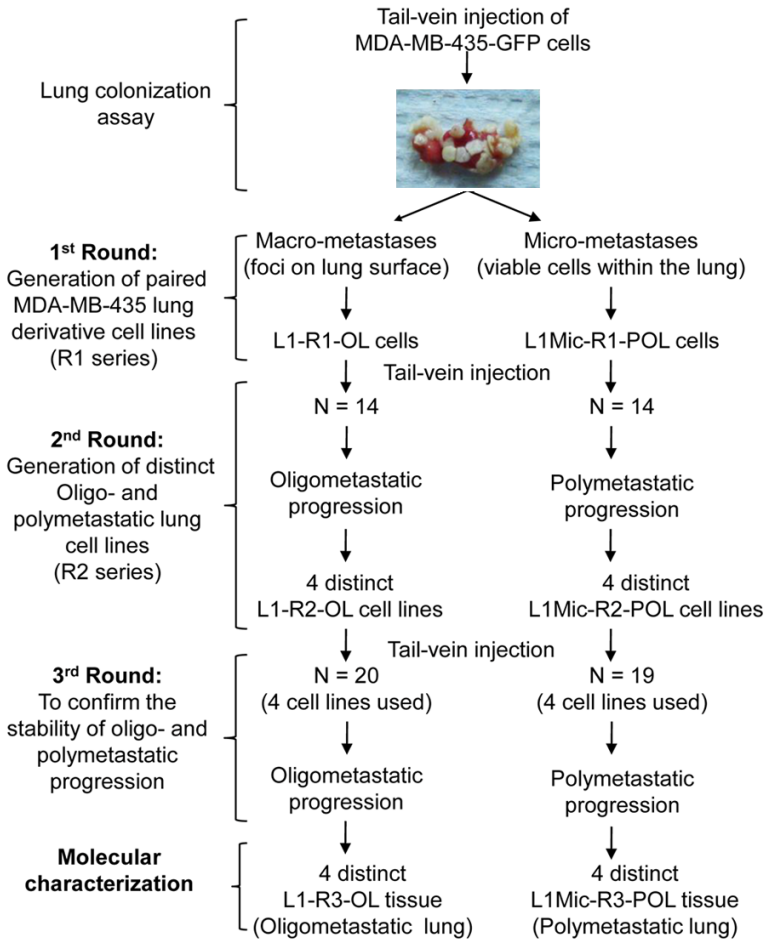

Figure 1. Experimental scheme of generation and *in vivo* characterization of metastatic MDA-MB-435-GFP lung derivative cell line series.

In order to study oligometastases as well as oligo- to poly-metastatic progression, we developed and characterized an oligometastases model of MDA-MB-435 human tumors in nude mice in which the clinical oligometastatic phenotype (≤ 5 total body macroscopic metastases) remained stable during consecutive *in vivo* characterization. In parallel, we also developed an MDA-MB-435 polymetastatic model in which the distribution of metastases demonstrated multiple foci in the lung, or involved more than five anatomic sites including lung, heart, muscle, peritoneal cavity, and pleura.

Materials and methods

Cell cultures

The ATCC origin of the parental MDA-MB-435-GFP cell line and its authentication was described in our recent study. MDA-MB-435 cells stably expressing green fluorescent protein (GFP) were generated as previously described [27, 28]. Cells were maintained in DMEM high glucose supplemented with 10% FBS + 200 μg/ml G418 (Gibco). Cells in the linear phase of growth in culture were harvested and prepared for intravenous tumor injection.

Generation of MDA-MB-435 lung oligometastatic (L1-OL) or polymetastatic (L1Mic-POL) sub-lines

All animal work was conducted in accordance with a protocol approved by the Institutional Animal Care and Use Committee (IACUC) at the Chongqing Medical University. Tail-vein injection of tumor cells and identification of polymetastatic animals over the course of 12 weeks. The number of lung metastases was determined by fluorescence imaging at necropsy. **Figure 1** summarizes the scheme we used to generate and characterize MDA-MB-435-based models of oligo- and polymetastases. Generation of lung derivative cell lines at each round of in vivo modeling was described in our recent study [12]. Briefly, we first produced paired cell lines derived from lung macrometastases (L1-R1-OL, L: lung, R1: Round 1 of *in vivo* modeling; OL: Oligometastatic) and micrometastases (L1Mic-R1-POL, L: lung; Mic: micrometastases; POL: polymetastatic). We define micro-metastatic foci as those that can only be identified by microscopic histological examination. In contrast, macro-metastatic foci are visible under external fluorescence imaging using Sellstrom Z87 fluorescence goggles and an LDP 470 nm bright blue flashlight. Subsequently, we established individual MDA-MB-435-GFP sub-lines from distinct lungs of oligo- and poly-metastatic animals injected with L1-R1-OL and L1Mic-R1-POL cells, respectively. All four oligometastatic L1-R2-OL (R2: Round 2

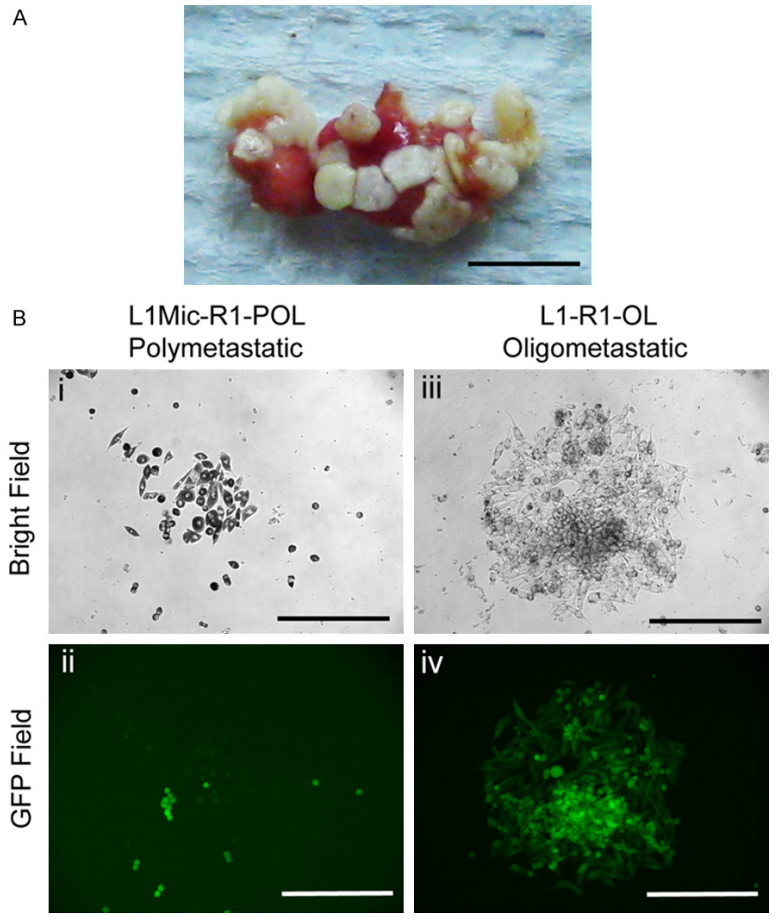

Figure 2. Development and characterization of MDA-MB-435-GFP xenograft models of oligo- and polymetastases. A. Polymetastatic lung used for establishing paired oligometastatic L1-R1-OL and polymetastatic L1Mic-R1-POL MDA-MB-435-GFP cell lines (scale bar, 0.5 cm). B. Isolation, purification and generation of oligometastatic L1-R1-OL (from macrometastses on the lung surface) and polymetastatic L1Mic-R1-POL cells lines (from dormant or micrometastases inside the lung) (scale bars, 200 μm).

of *in vivo* modeling) cell lines and four polymetastatic L1Mic-R2-POL cell lines will be used for future molecular characterization. Cell lines generated in the second round of *in vivo* modeling were tested for oligo- and polymetastatic progression in an additional round of *in vivo* testing [12].

Non-invasive in vivo whole-body fluorescence imaging of metastasis

The Olympus OV100 Small Animal Imaging System that affords variable magnification and high-resolution visualization capability from whole animal to a single cell was used for non-invasive imaging of tumor growth in live mice as we previously described [29-31]. 8-bit format images were acquired, converted into RGB color TIFF images using Image J, and imported into Photoshop in which contrast and brightness adjustment were applied to the whole image when necessary.

Histological analysis

Metastatic tissues harboring visible macro-metastases (including lungs, bone, muscle, heart, peritoneum, kidney) were excised and fixed in 10% formalin for 12 hours. Paraffin embedding, sectioning and H&E staining were performed for histological examination of the presence of both macro- and micro-metastases. Lungs were harvested from all animals. A total of 5 lungs from each treatment group were examined.

Statistical analysis

Statistical significance was assessed by unpaired two-tailed Student's t-test. $P< 0.05$ was accepted as statistically significant.

Results

Figure 1 summarizes the approach we used to generate and characterize the MDA-MB-435-based xenograft models of oligo- and polymetastatic progression. A general description of the incidence and time kinetics of metastasis of the oligo- and poly-metastatic lung cell lines summarized in **Figure 1**. Here, we provide a detailed characterization of distinct *in vivo* metastatic phenotypes of the oligo- and polymetastatic cell lines.

Development of oligometastatic and polymetastatic lung derivative cell lines

Green fluorescent protein (GFP) labeled MDA-MB-435 (435-P) cancer cells transplanted in the mouse fat pad develop a high incidence of spontaneous lung metastases [28-30]. We utilized the high lung colonization efficiency feature of this human tumor model to develop

Table 1. Characterization of metastatic outcome of L1-R1-OL and L1Mic-R1-POL MDA-MB-435-GFP lung derivative cell lines *in vivo* (the 2nd round of *in vivo* passage)

Cell Line	Mouse ID	Necropsy Observations											Tissue Harvest (wk)	Metastatic Phenotypes
		Brachial Plexus	Spinal Cord	Lumber Plexus	Xiphoid Process	Lymph Nodes	Lung Pleural	Brain	Skeletal Muscle	Peritoneum cavity	Urinary Duct	Liver		
L1-Mic-R1-MB-435-GFP (POL)	L1Mic-R1-#1						Dead*						<9	PL-M
	L1Mic-R1-#2						Dead*						<9	PL-M
	L1Mic-R1-#3						Dead*						<9	PL-M
	L1Mic-R1-#4	3	1	1	1	1ALN	++++++	No	+++++	No	1	No	9	PL-M
	L1Mic-R1-#5	1	1	1	1	1ALN 1CLN	++++++	1	+++++	+++	No	No	9	PL-M
	L1Mic-R1-#6	1	No	1	1	1ALN	+++++	No	+++++	No	No	No	9	PL-M
	L1Mic-R1-#7	1	No	1	No	1INL	+++++	No	+++++	+++	1	No	9	PL-M
	L1Mic-R1-#8	1	1	No	1	1ILN	+++++	No	+++++	No	No	No	9	PL-M
	L1Mic-R1-#9	No	No	No	No	No	No	No	No	No	No	No	12	N
	L1Mic-R1-#10	1	No	1	1	No	+++++	No	+++++	No	No	No	9	PL-M
	L1Mic-R1-#11	1	No	1	No	No	++	No	+++++	No	1	No	9	PL-M
	L1Mic-R1-#12	No	No	No	No	No	No	No	No	No	No	No	12	N
	L1Mic-R1-#13	No	No	No	No	No	No	No	No	No	No	No	12	N
	L1Mic-R1-#14	No	No	No	No	1CLN 2ALNs	+++++	No	No	No	No	No	9	PL-M
L1-R1-MB-435-GFP (OL)	L1-R1-#1	1	1	1	No	1ALN	+++++	No	No	No	No	No	10	PL-M
	L1-R1-#2	1	No	1	No	No	++	No	++	No	1	No	10	PL-M
	L1-R1-#3	1	No	No	No	1CLN	3	No	No	No	No	No	10	OL
	L1-R1-#4	No	No	1	No	No	No	No	No	No	No	No	11	OL
	L1-R1-#5	No	1	No	No	No	+++++	No	No	No	No	No	11	PL-M
	L1-R1-#6	No	No	No	No	No	No	No	No	No	No	No	12	N
	L1-R1-#7	No	No	No	No	No	No	No	No	No	No	No	12	N
	L1-R1-#8	No	No	No	No	1ALN	1	No	No	No	No	No	12	OL
	L1-R1-#9	No	No	1	No	No	No	No	1	No	No	No	12	OL
	L1-R1-#10	No	No	No	No	No	No	No	No	No	No	No	12	N
	L1-R1-#11	No	No	No	No	No	+++++	No	No	1	No	No	12	PL-L
	L1-R1-#12	No	No	No	No	No	No	No	No	No	No	No	12	N
	L1-R1-#13	No	No	No	No	No	1	No	No	No	No	No	12	OL
	L1-R1-#14	No	No	No	No	No	No	No	No	No	No	No	12	N

ALN: auxiliary lymph node; ILN: inguinal lymph node; CLN: cervical lymph node; POL-M: multi-organ polymetastases; POL-L: polymetastases at lung only; OL: oligometastasis(es); N: no metastasis; *: animals found dead in the cage and confirmed with multi-organ polymetastases at post mortal necropsy and no tissues were harvested for these animals; +: semi-quantitative assessment of polymetastases in an organ when the metastatic foci were diffused.

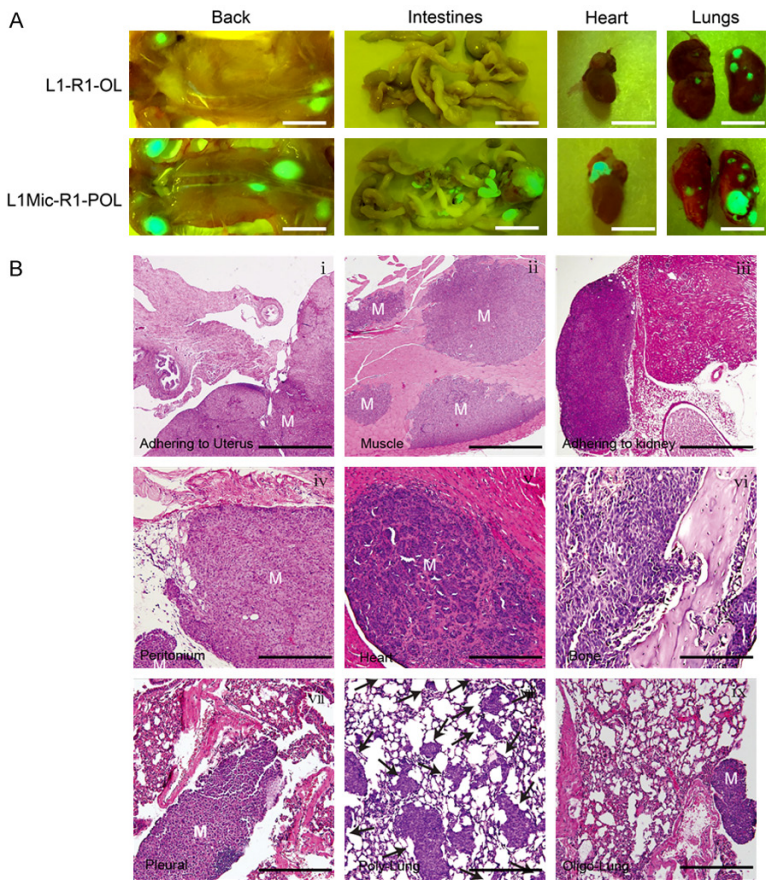

Figure 3. Widespread polymetastases in animals injected with L1Mic-R1-POL cells. A. OV-100 fluorescent imaging detected widespread polymetastases in animals injected with L1Mic-R1-POL cells. Shown is a representative animal that developed widespread polymetastases (scale bars, 1 cm). B. H&E characterization of polymetastases in different organs (scale bars, i-iii, 500 μm; iv-ix, 200 μm; M, metastasis).

stable MDA-MB-435-GFP xenograft models of oligometastatic and polymetastatic progression. Three consecutive rounds of lung colonization assays were performed in which lung and whole body macroscopic metastases were evaluated during the course of 12 weeks after tail vein injection of 2×10^6 cancer cells (**Figure 1** and Methods).

In order to minimize the extrinsic influence of the host tissue, such as mouse lungs, on metastatic progression, we isolated metastasizing MDA-MB-435-GFP cells, in the same animal, either from distinct macro-metastatic nodules on the lung surface (L1-R1-OL cells; L: lung, R1: Round 1 of *in vivo* modeling; OL: Oligometastatic) (**Figures 1** and **2A**) or from micro-metastases containing viable, slowly proliferating MDA-MB-435 cells within the lung parenchyma (L1-Mic-R1-POL cells; L: lung; Mic: micrometastases; POL: polymetastatic) (**Figures 1** and **2A**). L1-R1-OL and L1Mic-R1-POL MDA-435-GFP cells were recovered in culture with G418 selection to increase GFP expression (**Figure 2B**). The two resultant cell lines had distinct cellular morphology and growth rate. L1-R1-OL cells exhibited rapid cell proliferation and consisted of a mixture of small, round cells as well as larger, elongated cells (**Figure 2B**). In contrast, L1Mic-R1-POL cultured cells were mainly small, round, and morphologically less differentiated (**Figure 2B**). Expanded L1Mic-R1-OL cultures contained a mixture of both morphologically distinct cell types, though a significant portion of cells remain small and round and were either floating or loosely attached (data not shown). L1-R1-OL and L1Mic-R1-POL MB-435-GFP cells lines were used subsequently for developing oligometastases- and polymetastases-like xenograft models.

Development of stable in vivo models of oligo- and polymetastatic progression

We then tested whether the L1-R1-OL, and L1Mic-R1-POL MB-435-GFP cells remain metastatic in the lung colonization assay and whether they produce different patterns of metastases. Metastatic outcome and phenotype of each animal injected with either L1-R1-OL or L1Mic-R1-POL MDA-MB-435-GFP lung derivative cell lines in the second round of *in vivo* testing was summarized in details in **Table 1**.

Among 14 animals receiving L1-R1 cells, 10 developed either oligometastases or no metastases (**Table 1**, Oligometastases: defined as 5 or less, n=5; No metastases: n=5). Polymetastases (defined as more than 5 metastases) developed in 4 of 14 mice and occurred at 10-12 weeks post tumor cell injection. In contrast 11 of 14 mice receiving L1Mic-R1-POL cells devel-

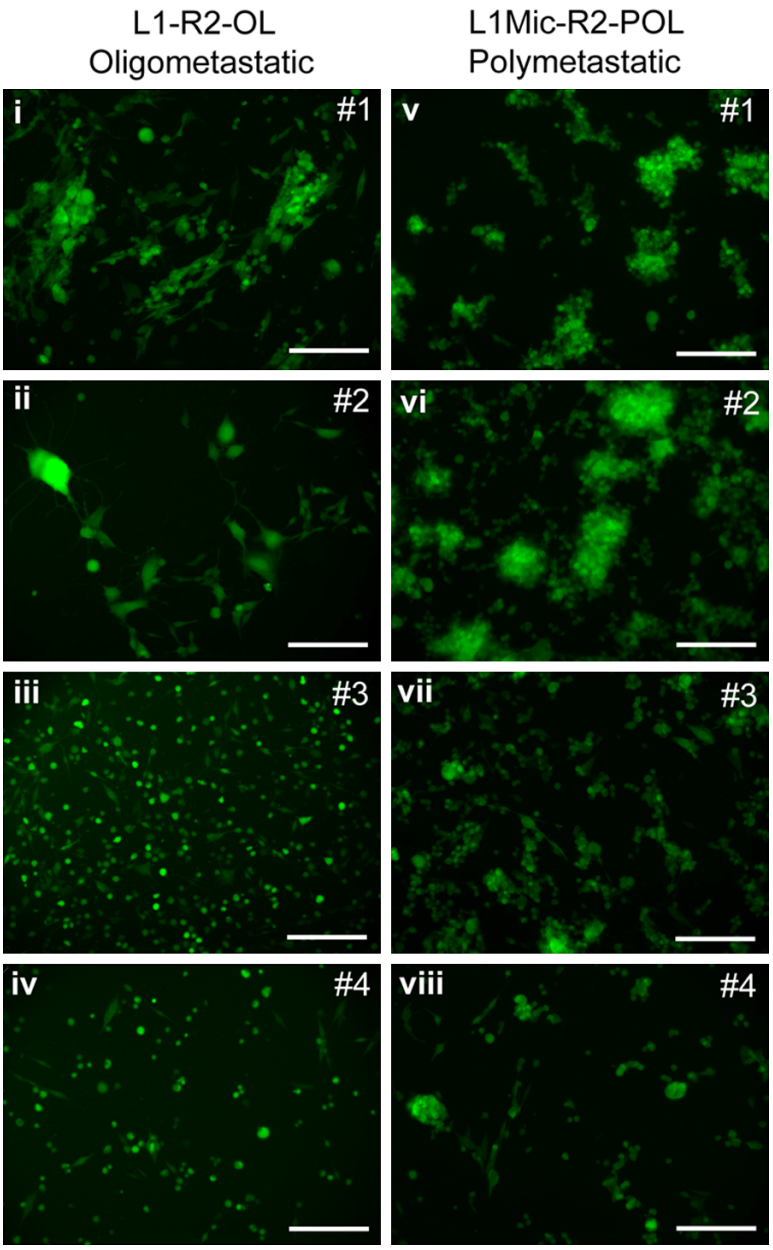

Figure 4. Generation of primary cell lines in the second round *in vivo* lung colonization assay. L1-R1-OL or L1Mic-R1-POL cells were injected via the tail vein. Metastasized L1-R1-OL or L1Mic-R1-POL cells to the lungs of oligometastatic and polymetastatic animals were isolated, respectively. Cancer cells were then recovered and expanded in culture. Four L1-R2-OL (i-iv) and four L1Mic-R2-POL cell lines (v-viii) were isolated for further *in vivo* testing (scale bars, 100 μm).

oped metastases, all of which were all polymetastases (**Table 1**). Polymetastases were either poly-foci in the lung (**Table 1**, POL-L: defined as >5 foci at lung only) or had multi-organ involvement in addition to lung polymetastases (**Table 1**, POL-M: >5 foci at lung and involved multi-organs). The time kinetics of metastasis in polymetastatic L1Mic-R1-POL cells was significantly faster than the oligometastatic L1-R1-OL cells. The faster progression to polymetastases in L1Mic-R1-POL cell injected animals was detected via non-invasive OV-100 fluorescent imaging (**Figure 3A**, Methods) [30, 31]. In addition to the high incidence of poly-foci metastases in the lungs as we previously reported [12], tail-vein injection of polymetastatic L1Mic-R1-POL cells also produced high frequency multi-organ metastases involving one or more of the following organs: muscle, peritoneal membrane and cavity, brain, bone, kidneys, heart and lymph nodes (**Figure 3B**). The involvement of specific organs in the multi-organ polymetastatic progression varied between animals. Thus, L1Mic-R1-POL cells appeared to be more polymetastatic-like contrasted with oligo-like L1-R1-OL cells. We next generated four oligometastatic L1-R2-OL (R2: Round 2 of *in vivo* modeling) lung cell lines (**Figure 4**), as well as four polymetastatic L1Mic-R2-POL lung cell lines (**Figure 4**) from eight animals of the second *in vivo* passage for further biological characterization.

Since *in vivo* passage of metastatic cancer cells usually enhances polymetastatic phenotype [20-23], we conducted an additional round of lung colonization experiments (the third round) to test the stability of L1-R2-OL and L1Mic-R2-POL cells in establishing oligometastases and polymetastases, respectively. Four L1-R2-OL and four L1Mic-R2-POL lung metastases-derived cell lines were used (**Table 2**). Among 19 mice that received the L1Mic-R2-POL cell lines (**Figure 4**), three failed to develop macroscopic metastasis. Of 16 animals that developed metastases, all had polymetastatic foci defined as in the lungs as well as in other

Table 2. Characterization of metastatic outcome of L1-R2-OL and L1Mic-R2-POL MDA-MB-435-GFP lung derivative cell lines *in vivo* (the 3rd round of *in vivo* passage)

Cell Line	Mouse ID	Necropsy Observations					Tissue Harvest (wk)	Metastatic Phenotypes
		Lung Pleural	Skeletal Muscle	Peritoneum cavity	Ovary	Other sites*		
L1Mic-R2-MB-435-GFP (POL)	L1Mic-R2-PL1-#1	++++	++++	++++	+++	4	6.5	PL-M
	L1Mic-R2-PL1-#2	++	++++	No	++++	No	6.5	PL-M
	L1Mic-R2-PL1-#3	No	No	No	No	No	12	N
	L1Mic-R2-PL1-#4	++++	No	No	No	No	12	PL-M
	L1Mic-R2-PL2-#1	++++	++++	No	No	4	6.5	PL-M
	L1Mic-R2-PL2-#2	++++	++++	No	+++	4	6.5	PL-M
	L1Mic-R2-PL2-#3	++++	+++	No	No	3	10	PL-M
	L1Mic-R2-PL2-#4	+++	No	No	No	1	11	PL-M
	L1Mic-R2-PL2-#5	++++	No	No	No	1	12	PL-M
	L1Mic-R2-PL3-#1	++++	++++	No	+++	3	7	PL-M
	L1Mic-R2-PL3-#2	+	++	No	++	1	8	PL-M
	L1Mic-R2-PL3-#3	++++	+++	No	++++	1	8	PL-M
	L1Mic-R2-PL3-#4	++++	No	No	+++	No	11	PL-M
	L1Mic-R2-PL3-#5	++++	No	No	+++	No	12	PL-M
	L1Mic-R2-PL4-#1	+++	++	++	No	2	6.5	PL-M
	L1Mic-R2-PL4-#2	++++	++++	No	+++	3	8	PL-M
	L1Mic-R2-PL4-#3	++++	++++	++++	++++	3	9	PL-M
	L1Mic-R2-PL4-#4	No	No	No	No	No	12	N
	L1Mic-R2-PL4-#5	No	No	No	No	No	12	N
L1-R2-MB-435-GFP (OL)	L1-R2-OL1-#1	+++	+++	No	++	3	6	PL-M
	L1-R2-OL1-#2	++++	No	No	No	No	9	PL-M
	L1-R2-OL1-#3	No	+++	++	+++	3	11	PL-M
	L1-R2-OL1-#4	4	No	No	No	No	12	OL
	L1-R2-OL2-#1	++++	++++	++	++++	4	7	PL-M
	L1-R2-OL2-#2	No	No	No	No	No	12	N
	L1-R2-OL2-#3	++++	+++	++	++	3	7	PL-M
	L1-R2-OL2-#4	++++	+++	No	No	3	7	PL-M
	L1-R2-OL2-#5	No	1	No	No	No	12	OL
	L1-R2-OL2-#6	No	No	No	No	No	12	N
	L1-R2-OL3-#1	++++	+++	No	++++	No	6	PL-M
	L1-R2-OL3-#2	No	No	No	No	No	12	N
	L1-R2-OL3-#3	1	No	No	+	No	12	OL
	L1-R2-OL3-#4	No	No	No	No	No	12	N
	L1-R2-OL3-#5	No	No	No	No	No	12	N
	L1-R2-OL4-#1	No	No	No	No	No	12	N
	L1-R2-OL4-#2	No	No	No	No	No	12	N
	L1-R2-OL4-#3	No	No	No	No	No	12	N
	L1-R2-OL4-#4	No	No	No	No	No	12	N
	L1-R2-OL4-#5	No	No	No	No	No	12	N

POL-M: multi-organ polymetastases; OL: oligometastasis(es); N: no metastasis; *: other sites include brachial plexus, spinal cord, lumber plexus and xiphoid process; +: semi-quantitative assessment of polymetastases in an organ when the metastatic foci were diffused.

organs (**Table 2**, POL-M). The widespread polymetastases could be detected before 7 weeks after tumor cell injection in 6 animals. In contrast of 20 mice injected with the L1Mic-R2-POL cell lines (**Figure 4**), 10 mice failed to develop visible macrometastases in any organ and 3 developed oligometastases examined at 12 weeks post tumor cell injection (**Table 2**). The differences were retained in this round of testing with respect to the incidence and the

extent of metastasis, the outcome of oligo- and polymetastases as well as the kinetics of establishing macro-metastases between the L1-R2-OL and L1Mic-R2-POL lung cell lines. Therefore, the differences between the two metastatic phenotypes were stably maintained *in vivo* over three successive passages.

Discussion

Mounting clinical observations begin to recognize oligometastases as a distinct clinical metastatic state where metastases are limited in number and destination organ [32-35] and oligometastases may represent a potentially curable subset of metastatic diseases [5, 6, 36]. However, only a subset of patients diagnosed with oligometastases will remain oligometastatic following treatment. Identification of this subset of patients at their initial presentation could help direct appropriate therapy.

Two models of tumor metastases have been proposed: the “late” and the “early” models of metastatic dissemination [37]. In the “late metastasis” model, late disseminating cells are genetically similar to the primary tumor. However, in the “early metastasis” model, the early metastatic tumor cells are genetically distinct from the non-disseminating tumor cells within the primary tumor. It is conceivable that the two models may not be mutually exclusive, and human solid tumors may employ both strategies in order to optimally progress and disseminate. Therefore, oligo- and polymetastatic state could be reached via both the early- or late models of metastases.

While various single organ-specific or spontaneous experimental models of metastases have been developed, they are selected for enhanced metastatic efficiency in contrast to the non-invasive or minimally invasive parental cancer lines or primary tumors [13-19]. Xenograft models of multi-organ polymetastases that resembles late-stage clinical metastatic dissemination are lacking. Prior to our study, animal models for human cancer oligometastases were not available. In order to investigate mechanisms underlying differences between oligometastases and polymetastases, we developed oligometastases and polymetastases models of the MDA-MB-435 human tumor in nude mice. These models have some unique features.

The oligometastatic phenotype of the L1-OL MDA-MB-435-GFP model remains stable *in vivo* after three consecutive rounds of passage (each round of testing lasted 12 weeks) and meets the clinical criteria of ≤ 5 total body macroscopic metastases. In contrast, metastatic efficiency of the existing metastasis models is invariably enhanced after *in vivo* selection [20-23], as also observed in our L1Mic-POL MDA-MB-435-GFP polymetastases model.

Tail-vein injection of polymetastatic L1Mic-R1-POL cells produced a high frequency of multi-organ metastases in the brain, peritoneal membrane and cavity, muscles, bone, kidneys, heart, and lymph nodes, with intramuscular metastases to the back and hind legs as the second most frequent event (**Figure 3A**, **3B**). Therefore, cells metastasized to organs other than lung likely have completed the full cascade of metastatic dissemination. The dissemination pattern of our polymetastatic MDA-MB-435-GFP breast cancer model while overlaps in part (lung, brain, bone, visceral) but is not identical to that observed in human breast cancer (**Table 1**). Most notably are the high incidence of muscle metastasis seen in our model that is uncommon in human cancer, and the lack of liver metastasis that is frequent in human breast cancer. Such discrepancies reflect differences in tumor cell and host microenvironment at the site of metastasis in mouse and in human. Nevertheless, the metastatic dissemination patterns of polymetastatic lung and multi-organ involvement are similar to clinical polymetastases.

Our models are optimized to demonstrate the differences in intrinsic properties that determine the outcome of oligo- or polymetastatic progression. Tissue microenvironment plays an important role in metastatic colonization [37-39]. We minimized the influence of individual differences in tissue microenvironment (in this case the mouse lung) on metastatic colonization, by isolating the paired oligometastatic L1-R1-OL cells and polymetastatic L1Mic-R1-POL cells from the lungs of the same animal, either from distinct nodules on the lung surface as (L1-R1-OL cells) or from viable cells within the lung parenchyma (L1Mic-R1-POL cells). Therefore, they were derived from same tissue microenvironment.

In summary, our study demonstrated the development and characterization of new xenograft models of metastases. They recapitulated phenotypic features of two clinically relevant human metastases phenotypes we identified: the oligometastatic and polymetastatic progression. These models should prove useful for mechanistic investigation as well as for evaluating therapeutic targeting of sustained oligometastases to achieve the clinical goal of long-term disease free survival.

Acknowledgements

This study was supported by grants from the Programs of National Natural Science of China (81272405, 81672908, 81602596).

Disclosure of conflict of interest

None.

Address correspondence to: Dr. H Rosie Xing, Laboratory of Translational Cancer Stem Cell Research, Chongqing Medical University, 1 Yi Xue Yuan Road, Yuzhong District, Chongqing, P.R. China. Tel: 023-68485106; Fax: 023-68486646; E-mail: xinglab310@163.com

References

[1] Staren ED, Salerno C, Rongione A, Witt TR and Faber LP. Pulmonary resection for metastatic breast cancer. Arch Surg 1992; 127: 1282-1284.

[2] Selzner M, Morse MA, Vredenburgh JJ, Meyers WC and Clavien PA. Liver metastases from breast cancer: long-term survival after curative resection. Surgery 2000; 127: 383-389.

[3] Fong Y, Cohen AM, Fortner JG, Enker WE, Turnbull AD, Coit DG, Marrero AM, Prasad M, Blumgart LH and Brennan MF. Liver resection for colorectal metastases. J Clin Oncol 1997; 15: 938-946.

[4] Tanvetyanon T, Robinson LA, Schell MJ, Strong VE, Kapoor R, Coit DG and Bepler G. Outcomes of adrenalectomy for isolated synchronous versus metachronous adrenal metastases in non-small-cell lung cancer: a systematic review and pooled analysis. J Clin Oncol 2008; 26: 1142-1147.

[5] Hellman S and Weichselbaum RR. Oligometastases. J Clin Oncol 1995; 13: 8-10.

[6] Weichselbaum RR and Hellman S. Oligometastases revisited. Nat Rev Clin Oncol 2011; 8: 378-382.

[7] Salama JK, Chmura SJ, Mehta N, Yenice KM, Stadler WM, Vokes EE, Haraf DJ, Hellman S and Weichselbaum RR. An initial report of a radiation dose-escalation trial in patients with one to five sites of metastatic disease. Clin Cancer Res 2008; 14: 5255-5259.

[8] Milano MT, Katz AW, Muhs AG, Philip A, Buchholz DJ, Schell MC and Okunieff P. A prospective pilot study of curative-intent stereotactic body radiation therapy in patients with 5 or fewer oligometastatic lesions. Cancer 2008; 112: 650-658.

[9] Rusthoven KE, Kavanagh BD, Burri SH, Chen C, Cardenes H, Chidel MA, Pugh TJ, Kane M, Gaspar LE and Schefter TE. Multi-institutional phase I/II trial of stereotactic body radiation therapy for lung metastases. J Clin Oncol 2009; 27: 1579-1584.

[10] Norihisa Y, Nagata Y, Takayama K, Matsuo Y, Sakamoto T, Sakamoto M, Mizowaki T, Yano S and Hiraoka M. Stereotactic body radiotherapy for oligometastatic lung tumors. Int J Radiat Oncol Biol Phys 2008; 72: 398-403.

[11] Hoyer M, Roed H, Traberg Hansen A, Ohlhuis L, Petersen J, Nellemann H, Kiil Berthelsen A, Grau C, Aage Engelholm S and Von der Maase H. Phase II study on stereotactic body radiotherapy of colorectal metastases. Acta Oncol 2006; 45: 823-830.

[12] Lussier YA, Xing HR, Salama JK, Khodarev NN, Huang Y, Hasselle MD, Zhang Q, Yang X, Khan SA, Malik R, Darga TE, Fan H, Perakis S, Filippo M, Lee Y, Posner MC, Chmura SJ, Hellman S and Weichselbaum RR. microRNA expression characterizes oligometastases Clinical Cancer Research 2011; Submitted, under consideration.

[13] Fidler IJ. Models for spontaneous metastasis. Cancer Res 2006; 66: 9787.

[14] Fidler IJ, Balasubramanian K, Lin Q, Kim SW and Kim SJ. The brain microenvironment and cancer metastasis. Mol Cells 30: 93-98.

[15] Fidler IJ and Kripke ML. Metastasis results from preexisting variant cells within a malignant tumor. Science 1977; 197: 893-895.

[16] Morikawa K, Walker SM, Nakajima M, Pathak S, Jessup JM and Fidler IJ. Influence of organ environment on the growth, selection, and metastasis of human colon carcinoma cells in nude mice. Cancer Res 1988; 48: 6863-6871.

[17] Nguyen DX, Bos PD and Massague J. Metastasis: from dissemination to organ-specific colonization. Nat Rev Cancer 2009; 9: 274-284.

[18] Sung V, Cattell DA, Bueno JM, Murray A, Zwiebel JA, Aaron AD and Thompson EW. Human breast cancer cell metastasis to long bone and soft organs of nude mice: a quantitative assay. Clin Exp Metastasis 1997; 15: 173-183.

[19] Bos PD, Nguyen DX and Massague J. Modeling metastasis in the mouse. Curr Opin Pharmacol 10: 571-577.

[20] Bruns CJ, Harbison MT, Kuniyasu H, Eue I and Fidler IJ. In vivo selection and characterization of metastatic variants from human pancreatic adenocarcinoma by using orthotopic implantation in nude mice. Neoplasia 1999; 1: 50-62.
[21] Morikawa K, Walker SM, Jessup JM and Fidler IJ. In vivo selection of highly metastatic cells from surgical specimens of different primary human colon carcinomas implanted into nude mice. Cancer Res 1988; 48: 1943-1948.
[22] Naito S, Walker SM and Fidler IJ. In vivo selection of human renal cell carcinoma cells with high metastatic potential in nude mice. Clin Exp Metastasis 1989; 7: 381-389.
[23] Poste G, Doll J, Hart IR and Fidler IJ. In vitro selection of murine B16 melanoma variants with enhanced tissue-invasive properties. Cancer Res 1980; 40: 1636-1644.
[24] Fidler IJ and Nicolson GL. Organ selectivity for implantation survival and growth of B16 melanoma variant tumor lines. J Natl Cancer Inst 1976; 57: 1199-1202.
[25] Fidler IJ and Nicolson GL. Tumor cell and host properties affecting the implantation and survival of blood-borne metastatic variants of B16 melanoma. Isr J Med Sci 1978; 14: 38-50.
[26] Fidler IJ. Selection of successive tumour lines for metastasis. Nat New Biol 1973; 242: 148-149.
[27] Li X, Wang J, An Z, Yang M, Baranov E, Jiang P, Sun F, Moossa AR and Hoffman RM. Optically imageable metastatic model of human breast cancer. Clin Exp Metastasis 2002; 19: 347-350.
[28] Zhang Q, Fan H, Shen J, Hoffman RM and Xing HR. Human breast cancer cell lines co-express neuronal, epithelial, and melanocytic differentiation markers in vitro and in vivo. PLoS One 5: e9712.
[29] Yamauchi K, Yang M, Jiang P, Xu M, Yamamoto N, Tsuchiya H, Tomita K, Moossa AR, Bouvet M and Hoffman RM. Development of real-time subcellular dynamic multicolor imaging of cancer-cell trafficking in live mice with a variable-magnification whole-mouse imaging system. Cancer Res 2006; 66: 4208-4214.
[30] Zhang Q, Yang M, Shen J, Gerhold LM, Hoffman RM and Xing HR. The role of the intravascular microenvironment in spontaneous metastasis development. Int J Cancer 2010; 126: 2534-41.
[31] Zhang Q, Bindokas V, Shen J, Fan H, Hoffman RM and Xing HR. Time-course imaging of therapeutic functional tumor vascular normalization by antiangiogenic agents. Mol Cancer Ther 10: 1173-1184.
[32] Rusthoven KE, Hammerman SF, Kavanagh BD, Birtwhistle MJ, Stares M and Camidge DR. Is there a role for consolidative stereotactic body radiation therapy following first-line systemic therapy for metastatic lung cancer? A patterns-of-failure analysis. Acta Oncol 2009; 48: 578-583.
[33] Mehta N, Mauer AM, Hellman S, Haraf DJ, Cohen EE, Vokes EE and Weichselbaum RR. Analysis of further disease progression in metastatic non-small cell lung cancer: implications for locoregional treatment. Int J Oncol 2004; 25: 1677-1683.
[34] Yoon SS and Tanabe KK. Surgical treatment and other regional treatments for colorectal cancer liver metastases. Oncologist 1999; 4: 197-208.
[35] House MG, Ito H, Gonen M, Fong Y, Allen PJ, DeMatteo RP, Brennan MF, Blumgart LH, Jarnagin WR and D'Angelica MI. Survival after hepatic resection for metastatic colorectal cancer: trends in outcomes for 1,600 patients during two decades at a single institution. J Am Coll Surg 210: 744-752, 752-745.
[36] Macdermed DM, Weichselbaum RR and Salama JK. A rationale for the targeted treatment of oligometastases with radiotherapy. J Surg Oncol 2008; 98: 202-206.
[37] Coghlin C and Murray GI. Current and emerging concepts in tumour metastasis. J Pathol 222: 1-15.
[38] Chaffer CL and Weinberg RA. A perspective on cancer cell metastasis. Science 331: 1559-1564.
[39] Chambers AF, Groom AC and MacDonald IC. Dissemination and growth of cancer cells in metastatic sites. Nat Rev Cancer 2002; 2: 563-572.